

AFRL-RW-EG-TP-2008-7409

MULTIFUNCTIONAL PARTICULATE COMPOSITES FOR STRUCTURAL APPLICATIONS (PREPRINT)

Jennifer L. Jordan
D. Wayne Richards
Air Force Research Laboratory
Munitions Directorate
AFRL/RWME
Eglin AFB, FL 32542-6810

Jonathan E. Spowart
Air Force Research Laboratory
AFRL/MLLMD
Wright Patterson AFB, OH 45433-7132

Bradley White
School of Materials Science & Engineering
Georgia Institute of Technology
Atlanta, GA 30332-0254

May 2008

CONFERENCE PAPER

This paper will be presented at the 2008 SEM XI International Congress and Exposition on Experimental and Applied Mechanics to be held in Orlando, FL on 2-5 June 2008. This paper will be published in the conference proceedings. One or more of the authors are U.S. Government employees working within the scope of their position; therefore, the U.S. Government is joint owner of the work. When published, the Society for Experimental Mechanics, Inc. may assert copyright. If so, the U.S. Government has the right to copy, distribute, and use the work by or on behalf of the U.S. Government. Any other form of use is subject to copyright restrictions.

This paper is published in the interest of the scientific and technical information exchange. Publication of this paper does not constitute approval or disapproval of the ideas or findings.

DISTRIBUTION A: Approved for public release; distribution unlimited.
Approval Confirmation 96 ABW/PA #03-17-08-158; dated 17 March 2008.



AIR FORCE RESEARCH LABORATORY, MUNITIONS DIRECTORATE

■ Air Force Materiel Command ■ United States Air Force ■ Eglin Air Force Base

REPORT DOCUMENTATION PAGE

*Form Approved
OMB No. 0704-0188*

The public reporting burden for this collection of information is estimated to average 1 hour per response, including the time for reviewing instructions, searching existing data sources, gathering and maintaining the data needed, and completing and reviewing the collection of information. Send comments regarding this burden estimate or any other aspect of this collection of information, including suggestions for reducing the burden, to Department of Defense, Washington Headquarters Services, Directorate for Information Operations and Reports (0704-0188), 1215 Jefferson Davis Highway, Suite 1204, Arlington, VA 22202-4302. Respondents should be aware that notwithstanding any other provision of law, no person shall be subject to any penalty for failing to comply with a collection of information if it does not display a currently valid OMB control number.

PLEASE DO NOT RETURN YOUR FORM TO THE ABOVE ADDRESS.

1. REPORT DATE (DD-MM-YYYY)		2. REPORT TYPE		3. DATES COVERED (From - To)	
4. TITLE AND SUBTITLE				5a. CONTRACT NUMBER	
				5b. GRANT NUMBER	
				5c. PROGRAM ELEMENT NUMBER	
6. AUTHOR(S)				5d. PROJECT NUMBER	
				5e. TASK NUMBER	
				5f. WORK UNIT NUMBER	
7. PERFORMING ORGANIZATION NAME(S) AND ADDRESS(ES)				8. PERFORMING ORGANIZATION REPORT NUMBER	
9. SPONSORING/MONITORING AGENCY NAME(S) AND ADDRESS(ES)				10. SPONSOR/MONITOR'S ACRONYM(S)	
				11. SPONSOR/MONITOR'S REPORT NUMBER(S)	
12. DISTRIBUTION/AVAILABILITY STATEMENT					
13. SUPPLEMENTARY NOTES					
14. ABSTRACT					
15. SUBJECT TERMS					
16. SECURITY CLASSIFICATION OF:			17. LIMITATION OF ABSTRACT	18. NUMBER OF PAGES	19a. NAME OF RESPONSIBLE PERSON
a. REPORT	b. ABSTRACT	c. THIS PAGE			19b. TELEPHONE NUMBER (Include area code)

Multifunctional Particulate Composites for Structural Applications

Jennifer L. Jordan, Air Force Research Laboratory, AFRL/RWMER, 2306 Perimeter Road,
Eglin AFB, FL 32542, jennifer.jordan@eglin.af.mil

Jonathan E Spowart, Air Force Research Laboratory, AFRL/RWLMD, Wright-Patterson AFB,
OH

Bradley White and Naresh N. Thadhani, School of Materials Science and Engineering, Georgia
Institute of Technology, Atlanta, GA 30332-0254

D. Wayne Richards, Air Force Research Laboratory, AFRL/RWME, Eglin AFB, FL 32542

ABSTRACT

Particulate composites consist of individual particles of one material dispersed throughout and held together by a polymer binder. The mechanical and physical properties of the composite depend on the mechanical and physical properties of the individual components; their loading density; the shape and size of the particles; the interfacial adhesion; residual stresses; and matrix porosity. Highly-loaded particulate composites are multi-phase systems that have not typically been studied rigorously, to date. We are investigating whether or not higher-order microstructural features can have a profound effect on the static and dynamic mechanical response of these multi-phase ($n > 2$) polymer-metal-ceramic composites. We present several models for the elastic and plastic behaviors of these materials, and compare the predictions with experimental data from quasi-static loading techniques. The high strain rate compressive properties, using a split Hopkinson pressure bar, of these materials are also characterized.

INTRODUCTION

Particulate composite materials composed of one or more varieties of particles in a polymer binder are widely used in military and civilian applications. They can be tailored for desired mechanical properties with appropriate choices of materials, particle sizes and loading densities. Several studies on similar epoxy-based composites have been reported and have shown that particle size [1, 2], shape [3], and concentration [4] and properties of the constituents can affect the properties of particulate composites. In composites of Al_2O_3 particles in epoxy (Epon 828/Z), increasing the particle concentration and decreasing the particle size were found to increase the stress at 4% strain [5]. A study of aluminum filled epoxy (DGEBA/MTHPA) found adding a small amount of filler (~ 5 vol.%) increased the compressive yield stress, but additional amounts of filler decreased the compressive yield stress [6]. However, tests on epoxy (DOW DER 331/bisphenol-A) found that increasing the volume percent of glass bead filler increased the yield stress and fracture toughness of the material [7, 8]. In a study on a similar material, decreasing the aluminum particle size from micro to nano resulted in increased epoxy crosslink density and subsequently increased static and dynamic strength [1]. In this study, a factorial design of experiments is used to examine the effect of aluminum particle size and aluminum and nickel volume fractions in epoxy-based Al-Ni particulate composites.

EXPERIMENTAL SET-UP

Composites of aluminum and nickel powders in an epoxy binder were prepared for this study. The aluminum particle size was varied between 5 (Valimet, H5 aluminum) and 50 (Valimet, H50 aluminum) μm . The H5 aluminum, shown in Figure 1(a), was found to have an average particle size of 5.43 μm with spherical smooth particles. The H50 aluminum particles, Figure 1 (b), were also smooth and nominally spherical with an average particle size of 51.91 μm . The nickel particles (Micron Metals) had rougher surface texture and more irregular shape shown in Figure 1 (c), with an average particle size of 47.45 μm . However, there was also a small fraction of particles in the powder that had an average particle size of 97.44 μm .

Proceedings of the 2008 SEM Annual Conference and Exposition on Experimental and Applied Mechanics

Distribution A: 96ABW/PA 03-17-08-158

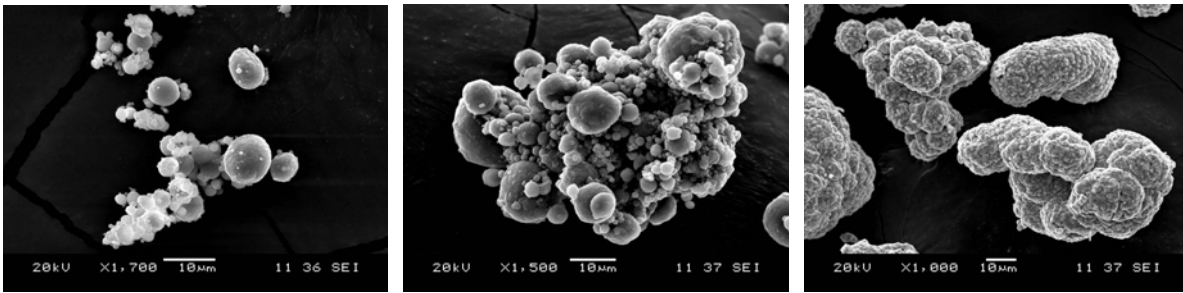


Figure 1: SEM micrographs of (a) H5 aluminum, (b) H50 aluminum and (c) nickel powders.

Table 1: Factorial design of experiments for epoxy-based particulate composites containing aluminum and nickel

Sample	Al Particle Size (µm)	Al Volume Fraction (%)	Ni Volume Fraction (%)
MNML-8	5	20	0
	5	20	10
	5	40	0
MNML-2	5	40	10
	50	20	0
MNML-3	50	20	10
MNML-5	50	40	0
	50	40	10

The composite materials used in this study were prepared using a fractional factorial design of experiments, with the variables being the aluminum particle size (5 or 50 µm), the volume fraction of aluminum (20 or 40 vol.%), and the addition of nickel (10 vol.%). The full factorial design of experiments is presented in Table 1, with the samples that were prepared highlighted.

Compression experiments at quasi-static strain rates were conducted with an MTS 810 testing system with a 100 KN test frame. Care was taken to center the samples on the platens prior to testing. MTS software was used to conduct constant true strain rate tests at $6.0 \times 10^{-4} \text{s}^{-1}$. A thin film of Boron Nitride (BN) with a layer of Molybdenum disilicide (MOSi_2) on top was used to lubricate the surfaces of the platen in contact with the test specimen. Prior to testing, the compression frame went through a warming up procedure of 600 cycles that oscillated the hydraulically driven ram at 1 Hz with a displacement around 2-3 in.

In addition to the MTS system recording the loads and displacement of the frame an interfacing software (VIC Gauge 2.0 from Correlated Solutions Inc.) reads input voltages for both the load and displacement. This software interfaces with a video system, which allows the user to place virtual displacement gages on the specimen that are tracked as testing takes place. A high contrasting boundary or point is required for tracking, and a black marker was used to draw fiducial marks on the specimens. The strain is measured directly from the specimen itself rather than from the MTS load frame. Multiple virtual displacement gages were used for comparison and to enable the test to continue in the event that one gage failed.

Compression experiments at intermediate strain rates (10^3s^{-1}) were conducted using a split Hopkinson pressure bar (SHPB) [9] system. The experiments were conducted using the SHPB system located at AFRL/RWME, Eglin AFB, FL, which is comprised of 1524 mm long, 12.7 mm diameter incident and transmitted bars of 6061-T6 aluminum. The striker is 610 mm long and made of the same material as the other bars. The samples, which were nominally 5 mm diameter by 2.5 mm thick are positioned between the incident and transmitted bars. The bar faces were lightly lubricated with grease to reduce friction.

The properties of the sample are determined by measuring the incident, reflected, and transmitted strain signals, ϵ_i , ϵ_R , and ϵ_T respectively, using Kulite AFP-500-90 semiconductor strain gages. These gages are smaller than traditional foil gages and have a much higher gage factor (140). The gages form part of a potential divider circuit with constant voltage excitation, which transforms the resistance change of the gages to a voltage change and compensates for temperature changes. The strain gages are dynamically calibrated in situ by performing a *Proceedings of the 2008 SEM Annual Conference and Exposition on Experimental and Applied Mechanics*

number of impacts with carefully measured striker bar velocities. From the measured impact velocity and mass of the striker, the force amplitude of the stress pulse introduced, F , can be determined and compared to the voltage output, V , from the strain gages to give a calibration in the form:

$$F = KV(1 + bV), \quad (3)$$

where K and b are calibration factors.

The full derivation of the data reduction used to calculate the strain rate and stress in the specimen, as functions of time, can be found in reference [9]. In order to make representative measurements of material properties, it is necessary that the specimen achieves mechanical equilibrium during the experiment, and this is sometimes assumed as it makes the strain rate calculation more straightforward [9]. The software used in the experiments presented in this paper performs the one- and two- wave analyses automatically for every specimen, so stress state equilibrium is verified in every experiment. However, the calculation of strain rate does not assume mechanical equilibrium, rather it uses all three of the incident, reflected and transmitted force pulses to calculate specimen strain rate through the following equation:

$$\dot{\varepsilon}(t) = \left[\frac{C_b}{l_s} \right] (\varepsilon_i(t) - \varepsilon_R(t) - \varepsilon_T(t)) \quad , \quad (4)$$

where ε_i , ε_R , and ε_T are the incident, reflected and transmitted strain pulses time shifted to the front and rear faces of the specimen, respectively, C_b is the sound speed in the bar material, and l_s is the length of the sample. This specimen strain rate is then integrated to give the strain,

$$\varepsilon(t) = \int_0^t \dot{\varepsilon}(t) dt \quad , \quad (5)$$

and the transmitted strain pulse is used to calculate the reported one-wave specimen stress,

$$\sigma(t) = \left[\frac{E_b A_b}{A_s} \right] \varepsilon_T(t), \quad (6)$$

where E_b , and A_b are the elastic modulus and cross-sectional area of the bar material, respectively, and A_s is the cross-sectional area of the sample. The two-wave specimen stress is calculated using Equation 6 with ε_T replaced by $\varepsilon_i + \varepsilon_R$. If true stress is required, A_s is typically updated using the strain calculation, assuming that volume is conserved during deformation.

In the quasi-static experiments, the elastic modulus was determined by fitting a straight line to the initial, linear part of the stress-strain curve. The yield stress, in both quasi-static and dynamic experiments, was determined by fitting a second order polynomial to the yield region of the stress-strain curve and taking the derivative to determine the maximum.

RESULTS AND DISCUSSION

Representative curves of the quasi-static compression results are shown in Figure 2 (a-d) in blue. It was found in these experiments that extreme care needed to be taken in order to center the samples on the load path to avoid shear failure in the materials. That the measured stress-strain curves in the quasi-static regime are serrated in nature is believed to be an artifact of the testing set-up rather than due to any intrinsic material property. The tests

Proceedings of the 2008 SEM Annual Conference and Exposition on Experimental and Applied Mechanics

were conducted under constant true strain conditions by continuously modulating the ram speed rate according to the measured force and ram displacement, in a feedback loop. Factors such as machine compliance and stick-slip loading on the compression specimen faces, along with any visco-elastic behavior of the epoxy matrix material can dramatically affect the control feedback to the ram, resulting in serrated loading curves. Similar serrations were not observed for the SHPB loading curves, which do not use this kind of feedback loop to effect true strain rate conditions. However, the overall trend in the stress-strain curve is a rise to peak stress followed by strain softening, more evident in MNML-3 and 5, which have a lower volume fraction of particulate, and subsequent strain hardening. This behavior is typical for polymer materials and has been observed in pure epoxy [10]. Additional testing using constant crosshead displacement is underway to confirm that the serrated nature of the stress-strain curve is due to the loading program rather than an intrinsic material behavior.

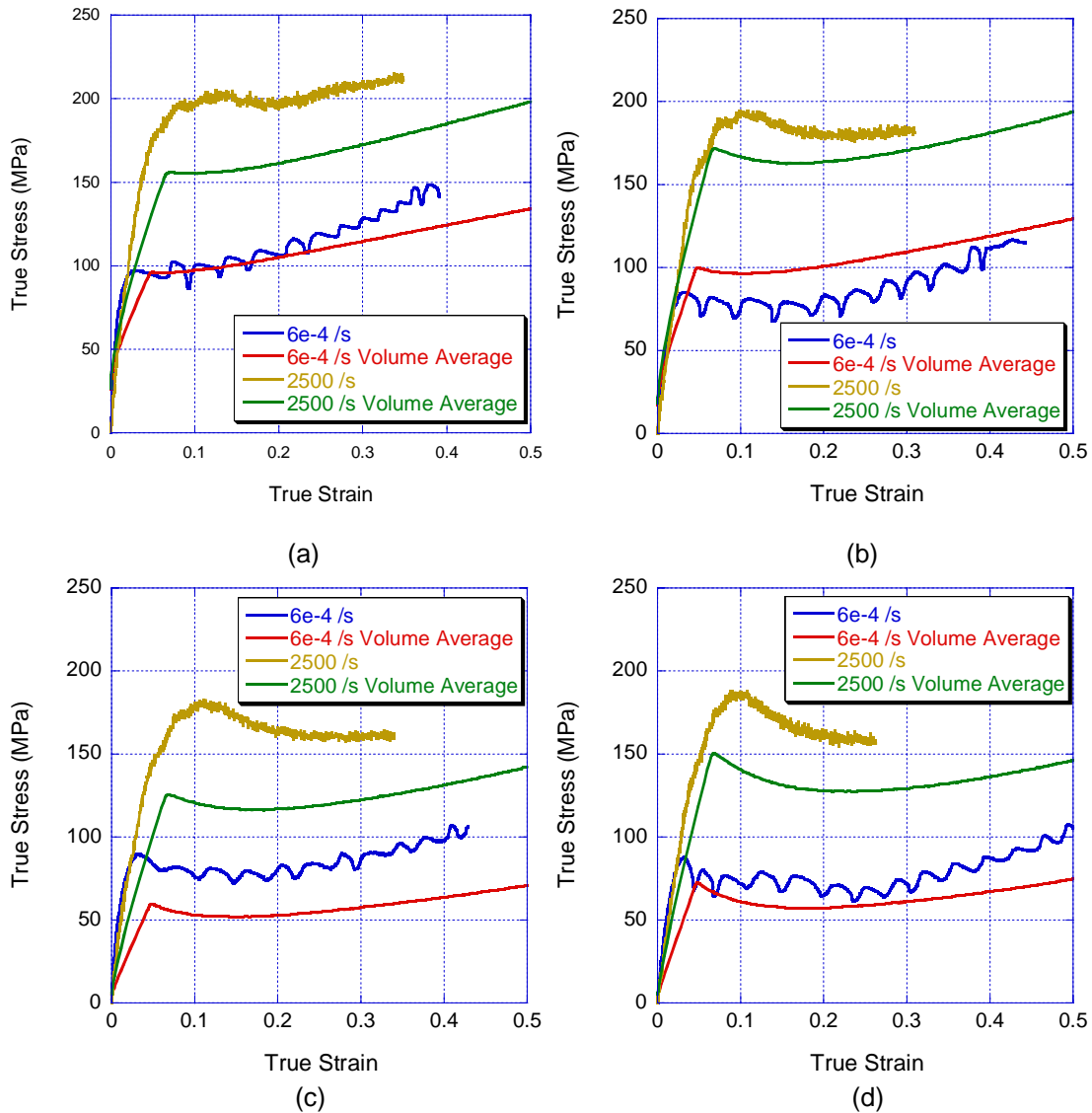


Figure 2: Stress-strain curves for (a) MNML-2, (b) MNML-3, (c) MNML-5, and (d) MNML-8. The volume average curves are determined from a volume average of the stress-strain curves calculated from the Mulliken-Boyce model fitted to epoxy [10], the Zerilli-Armstrong model for 99.99% pure aluminum [11] and the Johnson-Cook model for nickel 200 [12].

Each material was tested at 2500 /s using a split Hopkinson pressure bar, with representative curves shown in gold in Figure 2 (a-d). As discussed above, mechanical equilibrium in the samples needs to be verified, particularly in polymer based samples. Figure 3 (a-d) presents the one wave and two wave analyses for representative samples of all four materials, as well as the strain rate. It can be seen from this figure that all materials are in equilibrium by 5% strain. Due to the high volume fraction of particles, both Ni and Al, MNML-2 shows a different stress-strain response than the other composites. There is a lack of strain softening post-yield and instead strain hardening is observed, which is not present in the other samples.

The yield stress, defined in the experimental set-up section, for each material at both strain rates is plotted in Figure 4. If additional strain rates were measured, it would most likely be found, as is the case with epoxy, that there is a bilinear dependence of yield stress on strain rate due the beta phase transition in epoxy [10]. The percent increase of the yield stress with strain rate for the composites are approximately the same. MNML-3 exhibits a larger increase; however, since there are only two data points its difficult to conclude if this is real or due to variations in experimental measurements. Additional testing at several strain rates is underway to further elucidate the strain rate dependence of yield stress in these composite materials.

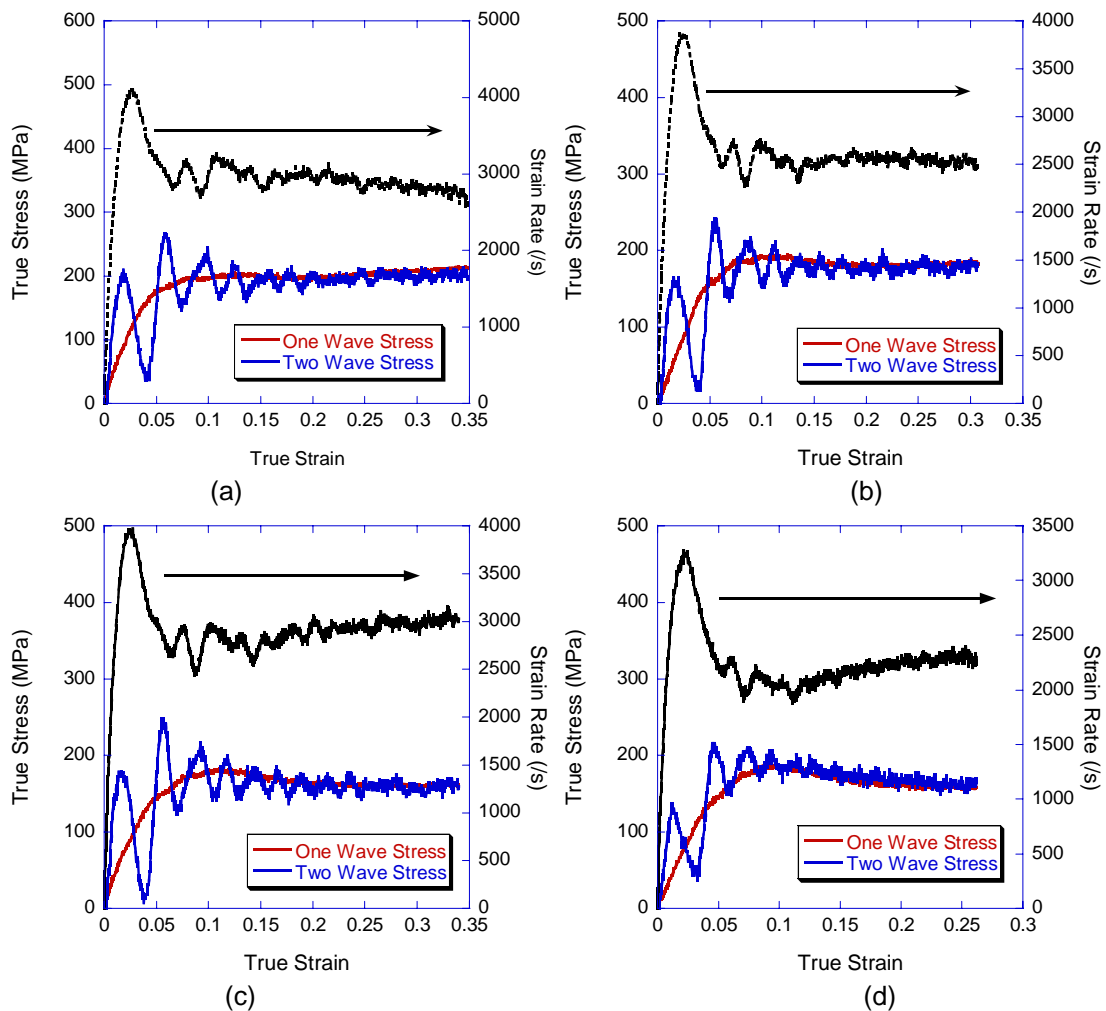


Figure 3: Comparison of one wave and two wave stresses as well as strain rate for (a) MNML-2, (b) MNML-3, (c) MNML-5 and (d) MNML-8.

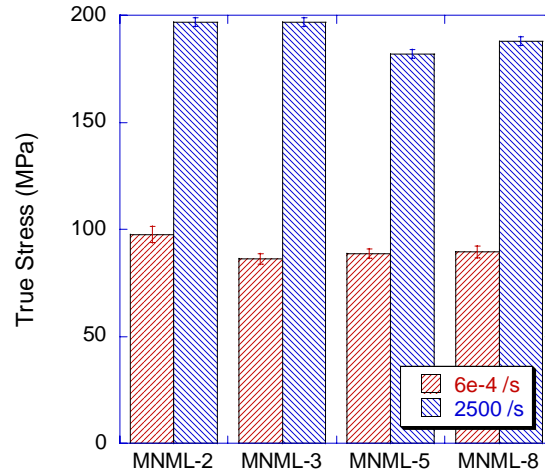


Figure 4: Strain rate dependence of yield stress for MNML-2, 3, 5, and 8.

Table 2: Mulliken-Boyce parameters for epoxy [10]

Variable	Units	Value
$E_{\alpha}(\theta, \dot{\epsilon})$	MPa	DMA data
$E_{\beta}(\theta, \dot{\epsilon})$	MPa	DMA data
$\nu_{\alpha}(\theta, \dot{\epsilon})$		0.38
$\nu_{\beta}(\theta, \dot{\epsilon})$		0.38
$\dot{\gamma}_{0,\alpha}$	s^{-1}	2.29×10^{15}
$\dot{\gamma}_{0,\beta}$	s^{-1}	2×10^6
ΔG_{α}	J	3.83×10^{-19}
ΔG_{β}	J	3.32×10^{-20}
$\alpha_{p,\alpha}$		0.316
$\alpha_{p,\beta}$		0.316
$s_{ss,\alpha}$	MPa	0.58
h_{α}	MPa	300
C_R	MPa	14.2
N	$m^{-1/2}$	2.3

A modeling approach was considered for predicting the properties of the composites from the properties of the individual components. In this method, a global volume average for each component, combined with a strength model for each component was used to determine a volume averaged stress-strain behavior. The volume fraction of each component was multiplied by the stress given by a constitutive equation for that component. Each of these was added together to obtain a volume averaged result. For epoxy, the Mulliken-Boyce model [13, 14] for glassy polymers was used with the parameters listed in Table 2 [10]. The equations defining this model are given in detail in [10, 13].

The Zerilli-Armstrong model [11] was used for pure aluminum, with the parameters presented in Table 3. In this model, based on the thermal activation of dislocation motion, the stress in FCC metals is given by

$$\sigma = c_0 + B_0 \epsilon^{1/2} \exp(-\beta T), \quad (7)$$

where

Table 3: Zerilli-Armstrong parameters for 99.99% pure aluminum [11]

Material	B_0 (MPa)	β_0 (K ⁻¹)	β_1 (K ⁻¹)	σ_G (MPa)	k (MPa*mm ^{1/2})
Aluminum (99.99%)	150	0.00089	0.000183	7	1.5

Table 4: Johnson-Cook parameters for nickel 200 [12]

Material	σ_0 (MPa)	B (MPa)	n	C	m	T_{melt} (K)
Nickel 200	163	648	0.33	0.006	1.44	1726

$$c_0 = \sigma_G + kl^{-1/2}, \quad (8)$$

$$\beta = \beta_0 - \beta \ln \dot{\epsilon}, \quad (9)$$

σ is the effective stress, ϵ is the effective strain, where a dot indicates the strain rate, σ_G is the stress contribution due the initial dislocation density, l is the grain size, k is the microstructural stress intensity, and B_0 , β_0 , and β_1 are constants. The aluminum particle size in the composites (5 or 50 μm) was used for the grain size term.

For the nickel component, the Johnson-Cook model [12] for nickel 200 was used with the parameters listed in Table 4. In this empirical model, multiplicative terms are used to describe the strain, strain rate, and temperature dependance

$$\sigma = [\sigma_0 + B\epsilon^n] [1 + C \ln \dot{\epsilon}^*] [1 - T^{*m}] \quad (10)$$

where σ_0 , B , C , n , and m are constants,

$$\dot{\epsilon}^* = \frac{\dot{\epsilon}}{\dot{\epsilon}_0} \quad (11)$$

with $\dot{\epsilon}_0 = 1$, and

$$T^* = \frac{T - T_r}{T_m - T_r} \quad (12)$$

where the subscript r refers to a reference temperature, typically room temperature, and the subscript m refers to the melt temperature.

The stress-strain curves calculated from volume averaging of the constitutive relationships for the component materials are shown in Figure 1, where the low strain rate is given by the red curve and the high strain rate is given by the green curve. For all the composites, the comparison at low strain rates is reasonably good for a first approximation. The low strain rate behavior of MNML-5 is underpredicted, which could be due to the equation of state for pure aluminum, which was used. The aluminum powder used in this study is 99.7% pure, compared with the 99.99% pure bulk aluminum used to develop the model. The volume averaged calculations underpredict the behavior in all of the composites at the high strain rates, indicating that there may be interactions at the high strain rates that are not taken into account purely by the high strain rate behavior of the components.

The samples prepared in this study were chosen as part of a half-factorial fractional design of experiments. As such, analysis can be conducted to determine the relative importance of each of the three variables, aluminum particle size and aluminum and nickel volume fractions, in determining the mechanical properties of the composite materials. Table 5 presents a summary of the quasi-static and dynamic yield stresses, the elastic modulus and the percent increase in stress from 6×10^{-3} /s to 2500 /s. A comparison of the significance of the three variables tested on the measured yield stress, elastic modulus and strain rate slope revealed that, as far as could be determined by the half-factorial experiments, they are equally important in determining the mechanical properties. Typically, a half-factorial design is not attempted for a system with only three variables. Additional work is *Proceedings of the 2008 SEM Annual Conference and Exposition on Experimental and Applied Mechanics*

underway to prepare samples for the remaining half of the factorial design in order to clarify the dependence of the mechanical properties on these experimental variables.

Table 5: Summary of mechanical properties of composite materials, where Vf is the volume fraction, σ_{ys} is the yield strength, and E is the elastic modulus.

	Al Particle Size (μm)	Vf Al	Vf Ni	σ_{ys} (MPa)	E (GPa)	σ_{ys} @ 2500/s (MPa)	% Increase in Stress
MNML-2	5	0.4	0.1	97.7	13.1	197	50.4
MNML-3	50	0.2	0.1	86.4	7.6	197	56.2
MNML-5	50	0.4	0	88.7	10.3	182	51.3
MNML-8	5	0.2	0	89.6	6.0	188	52.3

SUMMARY

This paper presented the compressive stress-strain behavior of epoxy-aluminum-nickel composites for two strain rates, prepared using a half-factorial design of experiments. Additional testing needs to be conducted to totally define the strain rate dependence of these materials. Two methods for modeling the mechanical response of the composites from the properties of the constituents were used. In the microstructure-based method, refined models for the component behavior, ex. a viscoelastic model for epoxy, need to be included in order to have better agreement with the experimental data. As a first approximation, the bulk volume averaging method showed good agreement with the low strain rate experiments. However, there was less agreement with high strain rate experiments indicating that there may be additional interactions taking place at high strain rates that are not accounted for by merely averaging the components. The significance of the three variables studied on the mechanical properties could not be determined using only a half-factorial design of experiments and additional samples are being prepared to accomplish a full factorial design.

ACKNOWLEDGEMENTS

This research was sponsored by the Air Force Office of Scientific Research (AFOSR/NA), Dr. Joan Fuller, Program Manager.

Opinions, interpretations, conclusions and recommendations are those of the authors and are not necessarily endorsed by the United States Air Force.

REFERENCES

1. Martin, M., S. Hanagud, and N.N. Thadhani, *Mechanical behavior of nickel + aluminum powder-reinforced epoxy composites*. Materials Science and Engineering: A, 2007. **443**(1-2): p. 209-218.
2. Ferranti, L. and N.N. Thadhani, *Dynamic mechanical behavior characterization of epoxy-cast Al + Fe₂O₃ thermite mixture composites*. Metallurgical and Materials Transactions A, 2007. **38A**(11): p. 2697-2715.
3. Ramsteiner, F. and R. Theysohn, *On the tensile behaviour of filled composites*. Composites, 1984. **15**(2): p. 121-128.
4. Ferranti, J.L., N.N. Thadhani, and J.W. House, *Dynamic Mechanical Behavior Characterization of Epoxy-Cast Al + Fe₂O₃ Mixtures*. AIP Conference Proceedings, 2006. **845**(1): p. 805-808.
5. Oline, L.W. and R. Johnson, *Strain rate effects in particulate- filled epoxy*. ASCE J Eng Mech Div, 1971. **97**(EM4): p. 1159-1172.
6. Goyanes, S., et al., *Yield and internal stresses in aluminum filled epoxy resin. A compression test and positron annihilation analysis*. Polymer, 2003. **44**(11): p. 3193-3199.
7. Kawaguchi, T. and R.A. Pearson, *The effect of particle-matrix adhesion on the mechanical behavior of glass filled epoxies: Part 1. A study on yield behavior and cohesive strength*. Polymer, 2003. **44**(15): p. 4229-4238.
8. Kawaguchi, T. and R.A. Pearson, *The effect of particle-matrix adhesion on the mechanical behavior of glass filled epoxies. Part 2. A study on fracture toughness*. Polymer, 2003. **44**(15): p. 4239-4247.
9. Gray III, G.T., *Classic split-Hopkinson pressure bar testing*, in *ASM Handbook Vol 8: Mechanical Testing and Evaluation*, H. Kuhn and D. Medlin, Editors. 2002, ASM International: Materials Park. p. 462-476.
10. Jordan, J.L., C.R. Siviour, and J.R. Foley, *Mechanical Properties of Epon 826/DEA Epoxy*. in preparation, 2008.
11. Zerilli, F.J. and R.W. Armstrong. *Constitutive Relations for the Plastic Deformation of Metals*. in *Shock Compression of Condensed Matter - 1993*. 1993: American Institute of Physics.

Proceedings of the 2008 SEM Annual Conference and Exposition on Experimental and Applied Mechanics

Distribution A: 96ABW/PA 03-17-08-158

12. Meyers, M.A., *Dynamic Behavior of Materials*. 1994, New York: John Wiley & Sons, Inc. 668.
13. Mulliken, A.D. and M.C. Boyce, *Mechanics of the rate-dependent elastic-plastic deformation of glassy polymers from low to high strain rates*. *International Journal of Solids and Structures*, 2006. **43**(5): p. 1331-1356.
14. Mulliken, A.D., et al., *High-rate thermomechanical behavior of poly(vinyl chloride) and plasticized poly(vinyl chloride)*. *Journal de Physique IV: JP*, 2006. **134**: p. 217-223.